Table 1 Numbers of patients and clinical practice in each institution

Institution	No. of patients				Cancer board	Salvage surgery	Median follow-up period of surviving patients (months)
	Group A	Group B	Group C	Total			
Nagoya Univ.	10	10	17	37 (1)	No	No	57
Niigata Univ.	16	12	17	45 (0)	No	No	56
Univ. Ryukyus	16	11	20	47 (1)	Yes	Yes	43
Kyoto Univ.	9	29	19	57 (2)	No	Yes	52
Kinki Univ.	7	17	42	66 (0)	Yes	Yes	69
Nara Med. Univ.	10	36	28	74 (1)	Yes	Yes	46
Hiroshima Univ.	38	15	26	79 (0)	Yes	Yes	70
Tenri Hospital	27	49	26	102 (2)	Yes	Yes	42
Tohoku Univ.	34	60	49	143 (3)	Yes	Yes	56
Total	167	239	244	650 (10)			

Values in parentheses indicate number of patients with non-squamous cell carcinoma histology

Group A, T1N0M0; Group B, T1N1M0,T2–3N0,1M0; Group C, T4,M1-lymph

Table 2 Treatment methods according to each institution between 1999 and 2003

Institution	Total no. of patients	Treatment for stage I			RT dose	Type of chemotherapy			
		CRT	RT	+IBT	Range (median)	Full FP	Low FP	Others	Consolidation
Nagoya Univ.	37	2	3	5	50–70 Gy (60 Gy)	1	19	11	No
Niigata Univ.	45	5	11	0	50–70.2 Gy (66 Gy)	1	22	11	No
Univ. Ryukyus	47	2	2	5	50–66.6 Gy (60 Gy)	28	4	0	No
Kyoto Univ.	57	2	2	5	60 Gy (60 Gy)	19	13	19	Some
Kinki Univ.	66	3	4	0	60 Gy (60 Gy)	11	51	0	Yes
Nara Med. Univ.	74	3	1	6	60–70 Gy (60.8 Gy)	10	58	0	No
Hiroshima Univ.	79	7	6	25	52–71 Gy (62 Gy)	16	15	19	No
Tenri Hospital	102	9	0	18	66 Gy (66 Gy)[a]	94	0	6	No
Tohoku Univ.	143	20	14	0	56–76 Gy (64 Gy)	57	23	49	Yes
Total	650	53	54	60 (21[b])		237	205	115	

[a] Hyperfractionation of 66/1.1 Gy b.i.d. was used

[b] Number of patients treated with CRT and IBT

intravenous infusion (IV) (days 1–4 or 1–5) [18–20], (2) two cycles of cisplatin 40 mg/m^2 (days 1 and 8) and 5-FU 400 mg/m^2/day as continuous IV (days 1–5 and 8–12) [6, 10], and (3) two or three cycles of cisplatin 60 mg/m^2 (day 1) and 5-FU 400 mg/m^2/day as continuous IV (days 1–4) [9, 21]. Low-dose FP included the following regimens: (1) two cycles of cisplatin 7 mg/m^2 (days 1–5 and 8–12) and 5-FU 250 mg/m^2/day as continuous IV (days 1–14) [5, 18, 19], and (2) six weekly cycles of cisplatin 3–5 mg/m^2 (days 1–5) and 5-FU 180–250 mg/m^2 as continuous IV (days 1–5 or 1–7) [19, 20, 22]. The other regimens included: (1) two cycles of *cis*-diammine-glycolatoplatinum (Nedaplatin) 55–80 mg/m^2 and 5-FU 300–700 mg/m^2 as continuous IV (days 1–5) [23], and (2) daily administration of 5-FU 300 mg/m^2/day as continuous IV for 6 weeks [7].

Two cycles of consolidation chemotherapy with cisplatin 70–80 mg/m^2 (day 1) and 5-FU 700–800 mg/m^2/day (days 1–4 or 1–5) were given after CRT at three institutions [10, 18]. No consolidation chemotherapy was given at the remaining six institutions.

Figure 1 shows the 3- and 5-year overall survival rates in the institutions for groups A, B, and C. The median and range of the 5-year overall survival rates of the nine institutions were 56% (48–83%) for group A, 29% (12–52%) for group B, and 19% (0–31%) for group C, respectively (Table 3). The 5-year overall survival rates for group A were good for all 9 institutions, although 56% of patients were treated by RT alone with or without IBT. A wide disparity in the 5-year overall survival rate was noted especially for group B.

The relationship between the number of patients treated per year and the 5-year overall survival rates of each

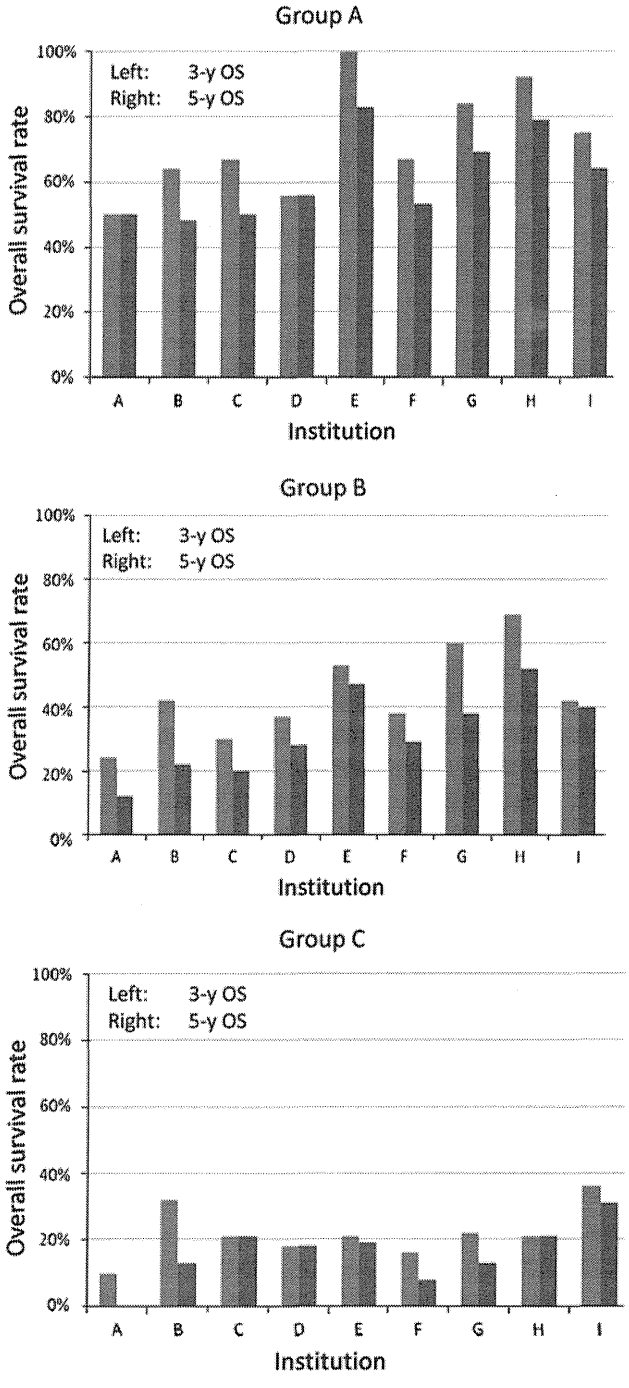

Fig. 1 The 3- and 5-year overall survival rates at each institution are shown for (**a**) group A, (**b**) group B, and (**c**) group C. The *left* and *right* columns are the 3- and 5-year overall survival rates of each institution, respectively

institution was analyzed for groups A, B, and C (Fig. 2). The correlation coefficient (r) and its 95% confidence interval for groups A, B, and C were 0.50 (−0.2455 to 0.8740), 0.70 (0.0602 to 0.9303), and 0.70 (0.0670 to 0.9312), respectively. A significant correlation between the number of patients treated per year and the 5-year overall

Table 3 The median and range of overall survival (OS) rates for patients with esophageal cancer treated between 1999 and 2003 at the 9 institutions

	3 years OS	5 years OS
Group A	67% (50–100%)	56% (48–83%)
Group B	42% (24–69%)	29% (12–52%)
Group C	21% (10–36%)	18% (0–31%)

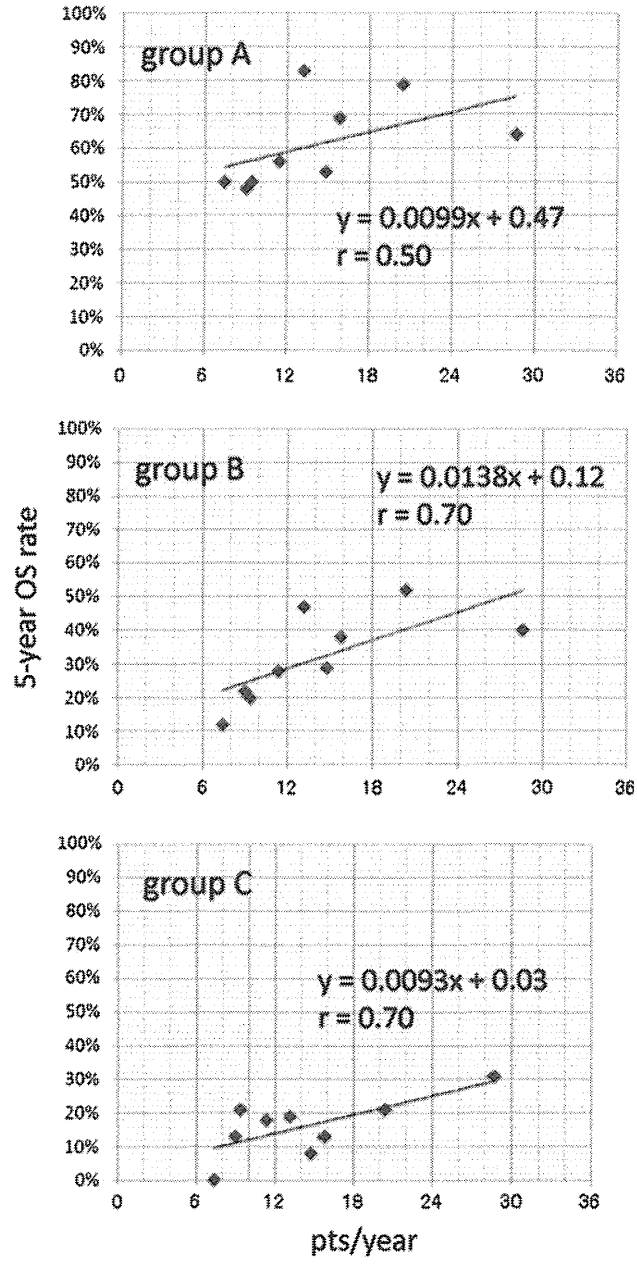

Fig. 2 Correlations between the number of patients treated per year (x-axis) and the 5-year overall survival rates of each institution (y-axis) for groups A, B, and C are plotted. The linear regression lines and correlation coefficients (r) for each group are shown

Table 4 Number of patients with serious late toxicities associated with CRT or RT

CTCAE version 3.0	Grade 3–4	Grade 5
Cardiac ischemia	1	3
Pericardial effusion	14	1
Pleural effusion	7	1
Radiation pneumonitis	4	2
Dysphagia	9	0
Hemorrhage, esophageal varices	1	0

survival rates was noted for groups B and C (both $p < 0.05$).

Based on the clinical charts of all patients, late toxicities of grade 3 or more (CTCAE version 3.0) were collected. The median and range of grade 3 or higher late toxicity rate for each institution were 11% (0–18%). Table 4 shows the number of patients with late toxicities of grade 3 or higher. Pericardial effusion and pleural effusion are most common late toxicities associated with CRT, followed by dysphagia and radiation pneumonitis. Although seven (1%) treatment-related deaths (grade 5) were reported, the deaths from cardiac ischemia may be coincidental.

Discussion

The present questionnaire-based survey revealed both clinical practice of care and outcomes for esophageal cancer treated by definitive RT or CRT in nine academic and major institutions between 1999 and 2003. The changes in clinical practice of RT for esophageal cancer in Japan have been well reported by the Japanese Patterns of Care Study (JPCS) [16, 17]. Based on the Comprehensive Registry of Esophageal Cancer in Japan for 2002, a total of 4,281 cases were registered from 222 institutions in Japan [24]. For cStage I–IIA (T1-3N0M0), the 5-year overall survival rates with concurrent CRT or RT alone were 52.0 and 32.5%, respectively. For cStage IIB–IVB, the 5-year overall survival rate with concurrent CRT was 14.9% [24]. However, no comparison of clinical outcomes of definitive RT or CRT at various institutions for esophageal cancer has been reported in Japan.

The JPCS between 1999 and 2001 revealed that CRT had become a common treatment for T2–4 esophageal tumors, although 72% of T1 tumors were treated by RT alone [16]. Therefore, clinical data for both RT alone and CRT were collected for stage I esophageal cancer (group A), although only data on CRT were collected for groups B and C. In the present analysis, 56% of the patients in group A were treated by RT alone and 44% were treated by CRT. Although the CRT rate for T1 tumors was higher than that in the JPCS between 1999 and 2001, more than half of T1 tumors were still treated by RT alone in Japanese academic and major institutions between 1999 and 2003. Following RT alone or CRT, 60 patients (36%) in group A were treated with IBT. The preference for IBT was heavily dependent on the institutional policy [9–12, 25].

For all institutions, medians of total RT dose for CRT ranged from 60 to 66 Gy. Although a total dose of 50.4 Gy combined with FP is the standard regimen for esophageal cancer in the USA, no institutions in this survey used a total dose of 50.4 Gy for definitive CRT. The type of chemotherapy differed significantly among the institutions. In Japan, low-dose protracted infusion chemotherapy combined with full-dose RT of 60–66 Gy used to be a popular regimen for locally advanced esophageal squamous cell carcinomas [5, 7, 16, 20, 22]. In the present analysis, full-dose FP was used most frequently (42.5%), followed by low-dose FP (36.8%) (Table 2). During this period, two clinical trials comparing full-dose FP and low-dose FP were performed at several institutions [18, 19]. In both trials, protracted low-dose FP with RT provided no advantage over standard short-term full-dose FP with RT for esophageal cancer. Low-dose FP will therefore decline in clinical practice in Japan.

The 5-year survival rates for stage I esophageal cancer exceeded 50% at most institutions, with a median 5-year survival rate of 56%. This survival rate seems excellent, as more than half of the patients were treated with RT alone. Thus, RT alone seems a definitive and effective treatment for elderly and complicated patients with superficial esophageal cancer.

One of the most notable findings in the present study was a significant disparity in overall survival rates among the institutions for patients with stage II–IVA disease treated definitively by CRT. The biggest difference in the 5-year overall survival rate was noted for group B. The highest 5-year overall survival rate of 52% was achieved at Tenri Hospital. At the hospital, definitive CRT was performed for responders to neoadjuvant CRT of 44 Gy/40 fractions, and surgery was performed for non-responders [9, 21]. This patient selection approach may be linked to the excellent survival rate. On the other hand, neither salvage surgery nor cancer board meetings were done for esophageal cancer at two hospitals showing poor 5-year survival rates of 12 and 22% for resectable esophageal cancer (Table 1). Thus, the disparity in overall survival rates may be related to the clinical practice at each institution.

A significant correlation between the number of patients treated per year and the 5-year overall survival rates was noted for groups B and C (both $p < 0.05$) (Fig. 2). A similar volume–outcome relation was demonstrated between the number of esophagectomy operations

performed per year and the operative mortality [26]. In terms of esophagectomy for cancer, a hospital with less than five esophagectomy operations per year was classified as a low-volume hospital with high operative mortality [26]. As the present series included only medium- and high-volume hospitals for CRT, survival rates by CRT at low-volume hospitals may be much lower than this series.

High rates of serious late toxicities, especially of the heart and pleura, associated with CRT have been reported [4, 27]. In this analysis, the median grade 3 or higher late toxicity rate of each institution was 11%. This late toxicity rate was considered acceptable, although it may have been underestimated due to the retrospective nature of the analysis.

In conclusion, the 5-year survival rates for stage I esophageal cancer were excellent, even with RT alone, at most institutions. However, for patients with stage II–IVA tumors treated definitively by CRT, a significant disparity in overall survival was noted among the institutions.

Acknowledgments This study was partially supported by a Grant-in-Aid for Scientific Research (21249066) from the Ministry of Education, Culture, Sports, Science and Technology, Japan, and a Grant-in-Aid from the Japanese Radiation Oncology Study Group (JROSG).

Conflict of interest None declared.

References

1. Al-Sarraf M, Herskovic A, Martz K et al (1997) Progress report of combined chemoradiotherapy versus radiotherapy alone in patients with esophageal cancer: an intergroup study. J Clin Oncol 15:277–284
2. Cooper JS, Guo MD, Herskovic A et al (1999) Chemoradiotherapy of locally advanced esophageal cancer: long-term follow-up of a prospective randomized trial (RTOG 85-01). Radiation Therapy Oncology Group. JAMA 281:1623–1627
3. Smith TJ, Ryan LM, Douglass HO Jr et al (1998) Combined chemoradiotherapy vs. radiotherapy alone for early stage squamous cell carcinoma of the esophagus: a study of the Eastern Cooperative Oncology Group. Int J Radiat Oncol Biol Phys 42:269–276
4. Minsky BD, Pajak TF, Ginsberg RJ et al (2002) INT 0123 (Radiation Therapy Oncology Group 94-05) phase III trial of combined-modality therapy for esophageal cancer: high-dose versus standard-dose radiation therapy. J Clin Oncol 20:1167–1174
5. Nishimura Y, Suzuki M, Nakamatsu K et al (2002) Prospective trial of concurrent chemoradiotherapy with protracted infusion of 5-fluorouracil and cisplatin for T4 esophageal cancer with or without fistula. Int J Radiat Oncol Biol Phys 53:134–139
6. Ohtsu A, Boku N, Muro K et al (1999) Definitive chemoradiotherapy for T4 and/or M1 lymph node squamous cell carcinoma of the esophagus. J Clin Oncol 17:2915–2921
7. Sakai K, Inakoshi H, Sueyama H et al (1995) Concurrent radiotherapy and chemotherapy with protracted continuous infusion of 5-fluorouracil in inoperable esophageal squamous cell carcinoma. Int J Radiat Oncol Biol Phys 31:921–927
8. Hironaka S, Ohtsu A, Boku N et al (2003) Nonrandomized comparison between definitive chemoradiotherapy and radical surgery in patients with T(2–3)N(any) M(0) squamous cell carcinoma of the esophagus. Int J Radiat Oncol Biol Phys 57:425–433
9. Murakami M, Kuroda Y, Nakajima T et al (1999) Comparison between chemoradiation protocol intended for organ preservation and conventional surgery for clinical T1–T2 esophageal carcinoma. Int J Radiat Oncol Biol Phys 45:277–284
10. Ariga H, Nemoto K, Miyazaki S et al (2009) Prospective comparison of surgery alone and chemoradiotherapy with selective surgery in resectable squamous cell carcinoma of the esophagus. Int J Radiat Oncol Biol Phys 75:348–356
11. Nishimura Y, Okuno Y, Ono K et al (1999) External-beam radiation therapy with or without high-dose-rate intraluminal brachytherapy for superficial esophageal cancer. Cancer 86:220–228
12. Sai H, Mitsumori M, Araki N et al (2005) Long-term results of definitive radiotherapy for stage I esophageal cancer. Int J Radiat Oncol Biol Phys 62:1339–1344
13. Nemoto K, Matsumoto Y, Yamakawa M et al (2000) Treatment of superficial esophageal cancer by external radiation therapy alone: results of a multi-institutional experience. Int J Radiat Oncol Biol Phys 46:921–925
14. Nemoto K, Yamada S, Hareyama M et al (2001) Radiation therapy for superficial esophageal cancer: a comparison of radiotherapy methods. Int J Radiat Oncol Biol Phys 50:639–644
15. Kato H, Sato A, Fukuda H et al (2009) A phase II trial of chemoradiotherapy for stage I esophageal squamous cell carcinoma: Japan Clinical Oncology Group Study (JCOG9708). Jpn J Clin Oncol 39:638–643
16. Murakami Y, Kenjo M, Uno T et al (2007) Results of the 1999–2001 Japanese patterns of care study for patients receiving definitive radiation therapy without surgery for esophageal cancer. Jpn J Clin Oncol 37:493–500
17. Kenjo M, Uno T, Murakami Y et al (2009) Radiation therapy for esophageal cancer in Japan: results of the Patterns of Care Study 1999–2001. Int J Radiat Oncol Biol Phys 75:357–363
18. Nishimura Y, Mitsumori M, Hiraoka M et al (2009) A randomized phase II study of cisplatin/5-FU concurrent chemoradiotherapy for esophageal cancer: short-term infusion versus protracted infusion chemotherapy (KROSG0101/JROSG021). Radiother Oncol 92:260–265
19. Sakayauchi T, Nemoto K, Ishioka C et al (2009) Comparison of cisplatin and 5-fluorouracil chemotherapy protocols combined with concurrent radiotherapy for esophageal cancer. Jpn J Radiol 27:131–137
20. Sai H, Mitsumori M, Yamauchi C et al (2004) Concurrent chemoradiotherapy for esophageal cancer: comparison between intermittent standard-dose cisplatin with 5-fluorouracil and daily low-dose cisplatin with continuous infusion of 5-fluorouracil. Int J Clin Oncol 9:149–153
21. Yamada K, Murakami M, Okamoto Y et al (2006) Treatment results of chemoradiotherapy for clinical stage I (T1N0M0) esophageal cancer. Int J Radiat Oncol Biol Phys 64:1106–1111
22. Sasamoto R, Sakai K, Inakoshi H et al (2007) Long-term results of chemoradiotherapy for locally advanced esophageal cancer, using daily low-dose 5-fluorouracil and *cis*-diammine-dichloroplatinum (CDDP). Int J Clin Oncol 12:25–30
23. Nemoto K, Matsushita H, Ogawa Y et al (2003) Radiation therapy combined with *cis*-diammine-glycolatoplatinum (Nedaplatin) and 5-fluorouracil for untreated and recurrent esophageal cancer. Am J Clin Oncol 26:46–49
24. Ozawa S, Tachimori Y, Baba H et al (2010) Comprehensive registry of esophageal cancer in Japan, 2002. Esophagus 7:7–22

25. Akagi Y, Hirokawa Y, Kagemoto M et al (1999) Optimum fractionation for high-dose-rate endoesophageal brachytherapy following external irradiation of early stage esophageal cancer. Int J Radiat Oncol Biol Phys 43:525–530
26. Fujita H, Ozawa S, Kuwano H et al (2010) Esophagectomy for cancer: clinical concerns support centralization operations within the larger hospitals. Dis Esophagus 23:145–152
27. Ishikura S, Nihei K, Ohtsu A et al (2003) Long-term toxicity after definitive chemoradiotherapy for squamous cell carcinoma of the thoracic esophagus. J Clin Oncol 21:2697–2702

Radiol Phys Technol (2013) 6:210–218
DOI 10.1007/s12194-012-0190-1

Dosimetric properties and clinical application of an a-Si EPID for dynamic IMRT quality assurance

Kenji Matsumoto · Masahiko Okumura · Yoshiyuki Asai · Kouhei Shimomura · Masaya Tamura · Yasumasa Nishimura

Received: 18 July 2012 / Revised: 19 November 2012 / Accepted: 20 November 2012 / Published online: 4 December 2012

Abstract Dosimetric properties of an amorphous silicon electronic portal imaging device (EPID) for verification of intensity-modulated radiation therapy (IMRT) were investigated as a replacement for conventional verification tools. The portal dosimetry system of Varian's EPID (aS1000) has an integrated image mode for portal dosimetry (PD). The source-to-imager distance was 105 cm, and there were no extra buildup materials on the surface of the EPID in this study. Several dosimetric properties were examined. For clinical dosimetry, the dose distributions of dynamic IMRT beams for prostate cancer (19 patients, 97 beams) were measured by EPID and compared with the results of ionization chamber (IC) measurements. In addition, pretreatment measurements for prostate IMRT (50 patients, 309 beams) were performed by EPID and were evaluated by the gamma method (criterion: 3 mm/3 %). The signal-to-monitor unit ratio of PD showed dose dependence, indicating ghosting effects. Tongue-and-groove effects were observed as a result of the dose difference in the measured EPID images. The results of PD for clinical IMRT beams were in good agreement with the predicted dose image with average values of 1.37 and 0.25 for γ_{max} and γ_{ave}, respectively. The point doses of PD were slightly, but significantly, higher than the results of IC measurements ($p < 0.05$ paired t test). However, this small difference seems clinically acceptable. This portal dosimetry system is useful as a rapid and convenient verification tool for dynamic IMRT.

Keywords Portal dosimetry · EPID · IMRT quality assurance

K. Matsumoto (✉) · M. Okumura · Y. Asai · K. Shimomura
Faculty of Medicine, Central Radiological Service,
Kinki University, 377-2 Ohno-higashi, Osaka-Sayama,
Osaka 589-8511, Japan
e-mail: kenji356@me.com

M. Tamura · Y. Nishimura
Faculty of Medicine, Department of Radiation Oncology,
Kinki University, Osaka-Sayama, Japan

1 Introduction

Advanced irradiation techniques, including intensity-modulated radiation therapy (IMRT), require extensive dose verification measurements. The delivery of IMRT beams employs several different techniques, including physical compensators, the step-and-shoot technique [1], and a dynamic multi-leaf collimator (MLC) [2–5]. Verification of dose distributions when these IMRT techniques are used requires at least two-dimensional (2D) dosimetry tools, and has been performed with use of radiographic film [6, 7]. This verification procedure includes recalculation of IMRT plans, set-up of radiographic films on linear accelerators, film processing and digitization, and comparisons of the calculated and measured dose distribution, which is a time-consuming procedure.

Amorphous silicon electronic portal imaging devices (a-Si EPID) were originally designed for patient set-up verification. Because portal images contain dosimetric information, The a-Si EPID has also been used for dose verification recently. 2D verification images can be acquired rapidly without re-entering of the treatment room. 2D detector dosimetry devices have also been proposed based on an ionization chamber or diode array for pretreatment verification of IMRT [8–11]. Whereas good agreement has been reported at specific points or along profiles, these two approaches have limited resolution (0.7–1.4 cm grid spacing) and require additional set-up

time. The EPID has the advantage of higher resolution, and it is already fixed to linear accelerators without needing any additional hardware. Because many radiotherapy departments have invested in portal imagers for patient set-up verification in recent years, it would be useful if the same device could be used also for accurate dose verification.

Early generations of EPIDs consisted of a liquid ion chamber and camera-based fluoroscopic units. The EPID images had poorer contrast and poorer spatial resolution than radiographic films [12–14]. The latest generation of EPIDs has an array of photodiode detectors on an amorphous silicon glass substrate (a-Si EPID). The a-Si EPID produces images that have improved spatial resolution and better contrast than the early generation EPIDs, because the device has an higher detective quantum efficiency.

The dosimetric properties of the a-Si EPID and its applicability to dynamic IMRT verification have been reported [15–21]. One of the approaches to EPID dosimetry was to convert an a-Si EPID image to a dose to water [22]. In this approach, Monte Carlo methods were applied for calculation of the predicted dose distribution at the plane of the EPID. Another approach was the back-projection method, which needs in-house programs for a-Si EPID dosimetry [23]. Each study explored the possibility of EPID dosimetry by use of a special in-house calculation algorithm.

Varian's portal dosimetry (PD) system has image acquisition hardware/software (IDU-20/IAS3) and does not need in-house software for calculation of the predicted dose image (PDI). This commercially available portal dosimetry system was commissioned for the quality assurance (QA) of IMRT treatment plans. Properties investigated were the linearity of the frame number, the linearity of the EPID signal-to-MU ratio, the influence of beam hold-off, the influence of MLC shapes, and the dose accuracy. As for clinical dosimetry, pretreatment verification for the prostate IMRT plan was performed by PD. Our aim in this study was to evaluate the dosimetric properties and application of the PD system as an IMRT verification tool.

2 Methods

An a-Si EPID (aS1000, Varian Medical Systems, Palo Alto, CA) consists of a 1 mm copper metal plate, a 134 mg/cm^2 gadolinium oxysulfide phosphor screen (Kodak, Lanex fast B) that includes a 0.18 mm polyester reflector and a 40 × 30 cm^2 (1,024 × 768 pixels) a-Si array. The 1 mm copper plate is equal to an 8-mm thickness of water and serves as buildup for the incoming radiation. The pixel pitch of aS1000 is 0.39 × 0.39 mm^2 at a source-to-image distance (SID) of 100 cm, which shows higher resolution than that of aS500. The aS1000 was equipped with a Varian 21EX linear accelerator (hereafter abbreviated as 21EX, Varian Medical Systems). 21EX has a Millennium 120 (60 pair) MLC system. Investigations of dosimetric properties and pre-treatment verification of the clinical IMRT plan were performed at an SID of 105 cm without extra buildup materials, with use of a 10 MV photon beam energy and a gantry angle of 0°. The SID of 105 cm is the measurement distance recommended by the manufacturer. The portal dose prediction (PDP) algorithm was implemented in the treatment planning system (TPS). We used the TPS (Varian Eclipse versions 7.3.10 and 10.0.24) to calculate the PDI. Recently, Eclipse was upgraded to version 10.0.24 from version 7.3.10. In the PD system, measured EPID dose images were compared with the PDI calculated from the fluence map of the clinical IMRT plan for verification of the IMRT plan.

2.1 Frame acquisition accuracy

For measurement of EPID dose images, Varian's EPID system uses an integrated image mode. In this study, EPID images were acquired by use of this mode. An EPID image was acquitted as a frame during irradiation. Accumulated frames were displayed as a single dose image after irradiation was completed. The preset rate of frame acquisition was 9.574 frames per second (fps) for 200–600 MU/min and 5.460 fps for 100 MU/min. The image acquisitions were controlled by the central processing unit (CPU) of image acquisition system version 3 (IAS3) located in the treatment room. To verify the accuracy of the frame acquisition by IAS3, we measured the frame number with MU set values of 1–999, and dose rate settings of 200 and 500 MU/min with a 10 × 10 cm^2 open field. For each MU setting, frame was continuously acquired during the irradiation, and they were quantified for each dose rate for analysis.

2.2 Accuracy of the EPID signal-to-MU ratio

The PD system requires several calibrations processes to be used as a dosimetric tool. The calibration procedure was performed according to a calibration protocol recommended by Varian Medical Systems. This calibration procedure has three steps, namely, acquisition of dark-field (DF) images, acquisition of flood-field (FF) images, and dose calibration. First, the DF image was acquired with no radiation and the pixel offsets were recorded. The FF image was recorded with an open-field irradiation (40 × 30 cm^2) for determination of the difference in sensitivity for each pixel. After the acquisition of DF and FF images, an absolute dose calibration was performed. The EPID signal was calibrated with irradiation delivery of 100 MU and a 10 × 10 cm^2 jaw setting. Each calibration

was performed with the dose rate of the verified IMRT plan. Because the PDI was calculated at an SID of 100 cm, a correction factor of 0.907 (i.e., inverse square of SID 105 cm) was applied to the measured EPID signal. The corrected EPID signal was converted to a calibration unit (CU). The CU is a unique absolute-dose unit of the PD (1 CU = 100 MU). The calibration procedure was performed routinely for every measurement.

To investigate the linearity of the signal-to-MU ratio in a range of 1–999 MU, we acquired EPID images using an open square field (10 × 10 cm^2). Two dose rates, 200 and 500 MU/min, were employed. CU values of EPID images were obtained as an average value of a 1 × 1 cm^2 region at the center of the irradiation field. As for the control, ionization chamber (IC) measurements were also performed with the same beam-delivery settings. The cylindrical IC used was a farmer type N30001 model (PTW, Hicksville, NY) of 0.6 cm^3 volume. The IC measurements were recorded in a water tank with the IC positioned at a 2.5-cm water depth and a source-detector distance (SDD) of 102.5 cm. To improve the signal-to-noise ratio, we performed IC measurements at a 2.5-cm water depth (d_{max} of 10 MV). These results were calculated as the signal-to-MU ratio and compared.

The essential factors for EPID-based dosimetry are accuracy of the imager calibration and that of the calculation algorithm of the PDI. To investigate the accuracy of the PDP algorithm, we also calculated the corresponding PDI. Because the PDI can be calculated only for dynamic IMRT fields, a 10 × 10 cm^2 jaw setting and a dynamic MLC moving outside the open field were employed. The CU values of the PDI were also measured as an average value of a 1 × 1 cm^2 area on the central axis. The measured and calculated CU values were compared.

2.3 Response to dose-rate fluctuations

The EPID was calibrated with a fixed dose rate similar to that of the original IMRT plan. When the MLC cannot reach a pre-defined position with maximum leaf speed, the accelerator reduces the dose rate until the MLC reaches a pre-defined position. This phenomenon causes large dose-rate fluctuations during IMRT beam delivery. This phenomenon may affect the measured EPID signals, because this portal dosimetry system is designed and calibrated under a stable dose-rate condition.

Effects of beam hold-offs were examined with use of a stepwise IMRT test pattern. We used two dose-rate settings of 100 and 600 MU/min to deliver the test field with 100 MU. The maximum leaf speed was 2.5 cm/s. Measurements at each dose-rate setting were performed under the same condition as that for the pre-treatment verification measurement. Two profiles along the leaf movement direction in the measured EPID images were obtained and compared.

2.4 Effect of MLC shapes

The MLC has several characteristics such as rounded-leaf-end and tongue-and-groove (T&G) shapes. Several studies investigated the specifications of MLC transmission [24, 25]. At our institution, the rounded-leaf-end transmission value was measured according to the method reported by Arnfield et al. and it was incorporated into the TPS as a calculation parameter. The T&G shape can reduce the transmission passing from each leaf side when the leaves are positioned side by side. However, if a single leaf side contributes to form a radiation field during IMRT irradiation, an unnecessary dose reduction may occur. To evaluate the effects of MLC characteristics on portal dosimetry, we examined a test field using a step-and-shoot

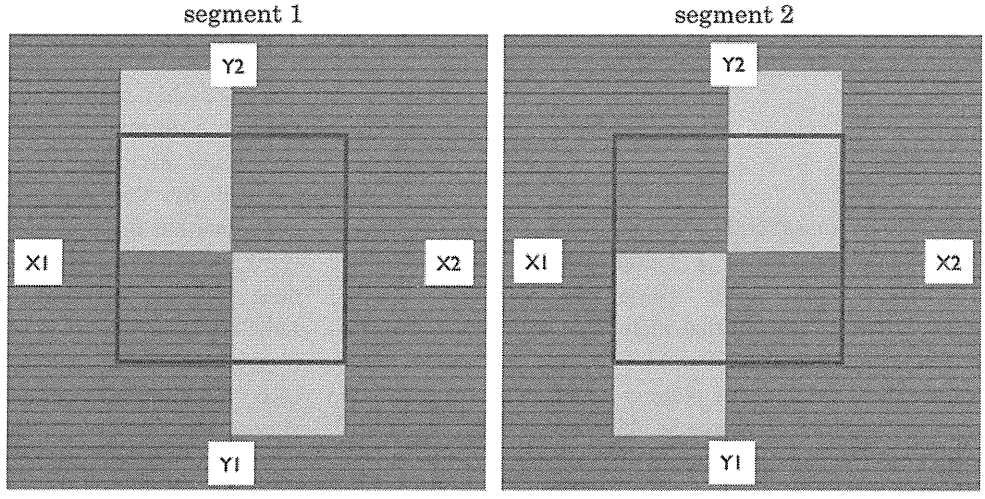

Fig. 1 MLC settings for test fields with 10 × 10 cm^2 jaw sizes. Two segments of MLC were delivered with use of a step-and-shoot IMRT technique

IMRT technique. Two MLC segments were planed sequentially in step-and-shoot mode. The leaf settings of the two segments are shown in Fig. 1. The test field was measured with 100 MU and divided into 50 MU for each segment similar to the pre-treatment verification condition. The PDIs were also calculated by the PDP algorithm of both versions 7.3.10 and 10.0.24. Two dose profiles parallel and perpendicular to the movement direction of the MLC were measured and compared with the PDI.

2.5 Dose accuracy of portal dosimetry

To apply the PD system as a reliable dosimetric tool, it is necessary to confirm whether it has an accuracy equivalent to that of the traditional verification tool. Pre-treatment verification of 19 clinical IMRT plans (97 beams) was performed by EPID and IC. The clinical IMRT plans for the prostate were calculated with use of a dynamic MLC technique, with 5–7 beams of 10 MV X-rays. These were planned by use of a pencil-beam convolution algorithm and a 300 MU/min dose rate so that beam hold-off was avoided. A Farmer type N30001 model (PTW, Hicksville, NY) of 0.6-cm^3 volume was used. To calculate the IC dose, we obtained CT images of a homogeneous IMRT phantom with IC. Each IMRT beam was transposed into the CT image within the TPS. The IC was positioned at high-dose areas in the IMRT dose distribution for improvement of the signal-to-noise ratio. Each IMRT field was recalculated with a gantry angle of 0° and with the same number of MUs as in the original IMRT plan. IC measurements were performed at the same calculation position. The ratio between the IC-measured dose (IC_{meas}) and the TPS-calculated dose ($Plan_{calc}$) was calculated. After EPID calibrations, PD measurements were performed. A point dose on the EPID image was selected at the same position as that of the IC. For every IMRT plan, the verification plan was recalculated by use of PDP algorithm version 7.3.10. The measured EPID doses were compared with the PDI doses. The ratio between the EPID-measured dose ($EPID_{meas}$) and the PDI-calculated dose (PDI_{calc}) was calculated for each beam. Finally, ratios of dose differences for ΔEPID (ΔEPID = $EPID_{meas}/PDI_{calc}$) and ΔIC (ΔIC = $IC_{meas}/plan_{calc}$) were compared and analyzed.

2.6 Clinical application

Pre-treatment verification of 50 prostate IMRT plans with 309 beams was performed by PD. EPID dose images were measured at a gantry angle set to 0° with the original MU. The PDIs were calculated by PDP algorithm version 7.3.10. The measured and calculated dose images were compared by use of the gamma analysis function provided in the Eclipse software [26]. Comparison criteria were set

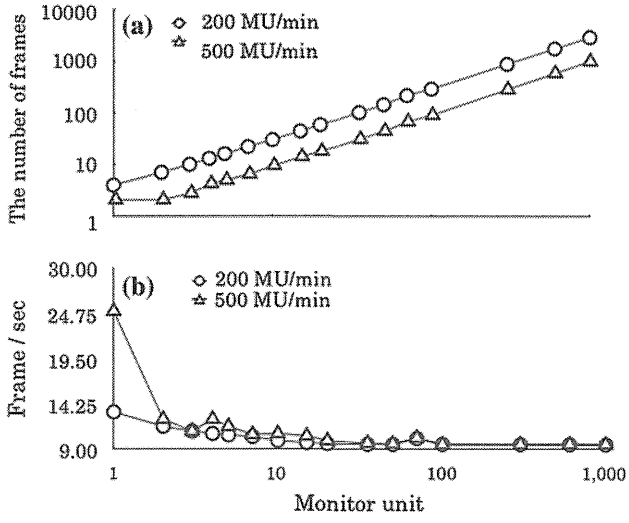

Fig. 2 **a** Linearity of acquired frame number with the monitor unit. Dose rates selected were 200 and 500 MU/min. **b** Frame acquisition rate calculated from the frame number. Preset value of the frame acquisition rate was set as 9.574 fps for each dose rate

to ±3 % for dose difference and ±3 mm for distance to agreement. The 10 % threshold of the maximum dose was utilized. Maximum gamma (γ_{max}) and average gamma (γ_{avg}) values of 309 IMRT beams were analyzed.

3 Results

3.1 Frame acquisition accuracy

The relationship between the number of frames and the MUs delivered is shown in Fig. 2a. Below 3 MU of 500 MU/min, the acquisition frame number per MU was not linear. The frame/s increased up to 25.0. However, this increase in fps was observed only below 3 MU and in high-dose-rate (500 MU/min) beam-delivery situations. The acquisition frame number per MU was stable at 3 MU or more for both dose rates (Fig. 2b).

3.2 Accuracy of the signal-to-MU ratio on EPID

Figure 3 shows signal/MU ratios for EPID and IC. Each ratio was normalized at 100 MU. The signal/MU ratio decreased from 1.0 at MUs of <70. At a high dose rate of 500 MU/min, this tendency was more apparent. In contrast, signal/MU ratios were stable at all MUs for IC. The ghosting effect was observed in the EPID results, and the dependence on the dose rate was identified.

Results for the PDP algorithm calculation accuracy are shown in Fig. 4. The percentage dose differences between measured and calculated CU values were within ±0.5 % at 100 MU or more. Measured CU values of <70 MU were systematically below the calculated CU value. Eventually, in

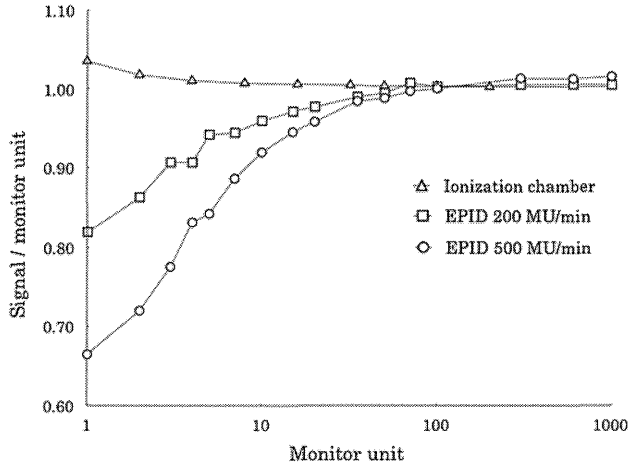

Fig. 3 Signal-to-monitor unit ratios measured by EPID and an ionization chamber. The ionization chamber reading was recorded for determination of the delivery system stability. Each curve was normalized to 1.0 at 100 MU

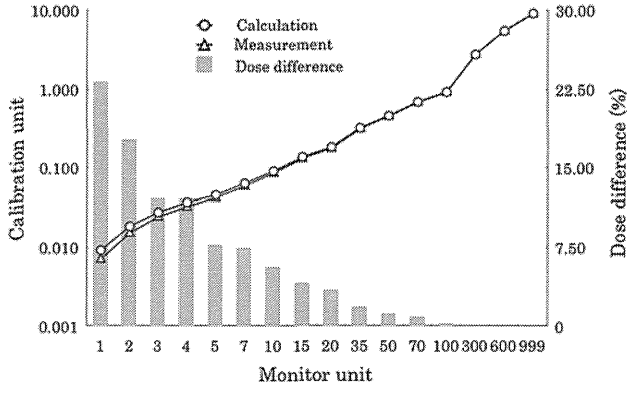

Fig. 4 Calculation accuracy of the PDP algorithm compared with measurements. Dose differences between calculation and measurement are shown as a *bar graph*

PD, combination of ghosting effect and PDP algorithm calculation accuracy was effective on the situation of small MU delivery.

3.3 Response to dose-rate fluctuations

Measured profiles of a test pattern are shown in Fig. 5. The leaf speeds and dose rate were stable during irradiation at 100 MU/min. At a dose rate of 600 MU/min, the dose rate fluctuated between 130 and 600 MU/min when the leaf speed reached 2.5 cm/s. This phenomenon may also occur in clinical IMRT plans. There was no difference in measured CUs at the two different dose rates.

3.4 Effect of MLC shapes

Measured EPID images for the two MLC segments delivered sequentially in step and shoot modes are shown in

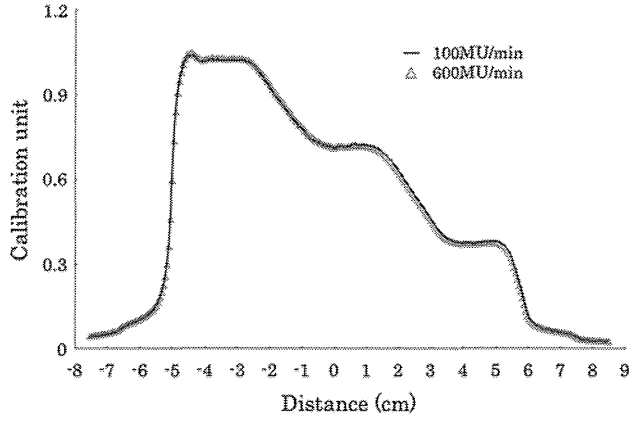

Fig. 5 Effect of dose-rate fluctuations during intensity modulated beam delivery. The stepwise test pattern was delivered by 100 MU at 100 and 600 MU/min. There was beam hold-off during beam delivery of 600 MU/min

Fig. 6a. The leaf settings of the two segments are shown in Fig. 1. Profiles perpendicular (inline) and parallel (crossline) to the leaf movement direction are shown in Fig. 6b and c, respectively. Each profile was compared with the calculation by the PDP algorithm. Versions of the PDP calculation algorithm used were 7.3.10 and 10.0.24. On the crossline profile, the dose discrepancy between measured and calculated values for versions 7.3.10 and 10.0.24 was 2.0 and 0.4 %, respectively. The location of this discrepancy just corresponded to the leaf end. This result indicates that the rounded leaf end value employed at our clinic seems correct and was calculated accurately. For the inline profile, calculation of PDP version 7.3.10 did not reflect the T&G effects, and the calculated dose exceeded 21 % of the measured dose (1.4 γ_{max} value). However, with the latest PDP version, 10.0.24, the T&G effect could be calculated.

3.5 Dose accuracy of portal dosimetry

Point dose differences between PD and IC measurements for 19 prostate IMRT plans with 97 beams are shown in Fig. 7. A positive number indicates that the measured dose was higher than the calculated values. The averaged values of ΔIC and ΔEPID were 0.5 $\pm$ 0.9 % (average $\pm$ SD) and 1.4 $\pm$ 1.0 %, respectively. ΔEPID was systematically and significantly higher than ΔIC ($p < 0.05$, paired t test).

3.6 Clinical application

Histograms of average and maximum γ values for all 309 IMRT beams are shown in Fig. 8. Good agreement between the predicted and measured dose images was observed when we used the 3 mm and 3 % γ criteria. The 10-% threshold was enough to take into account the ghosting effect, because that effect acted on the low-dose

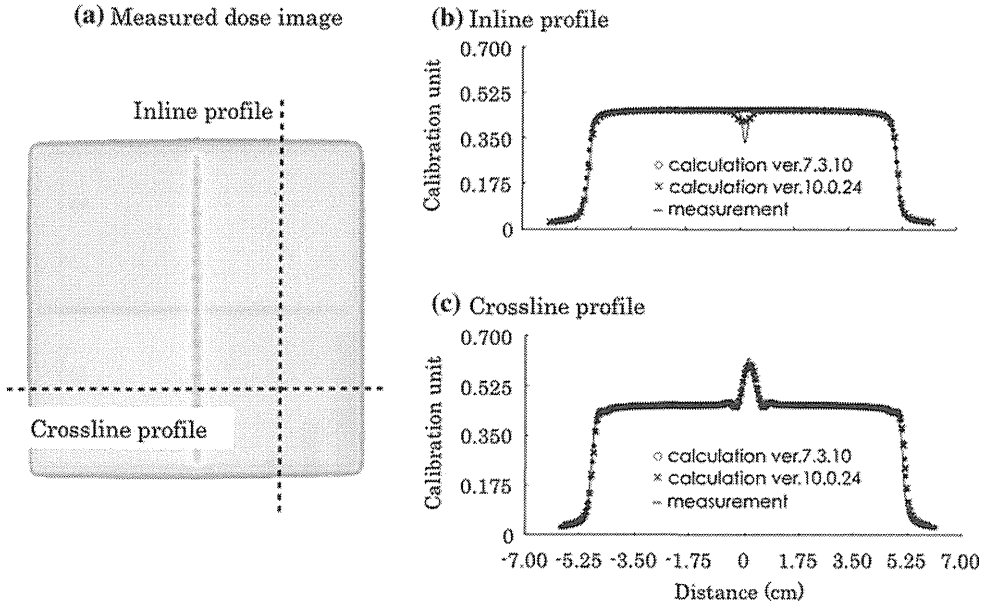

Fig. 6 MLC commissioning test of the PDP calculation algorithm. Two versions were used, 7.3.10 and 10.0.24. **a** Measured dose image of the test IM beam by use of Fig. 1 MLC pattern. **b** Result of inline profile comparing calculated and measured values. **c** Result of crossline profile comparing calculated and measured values

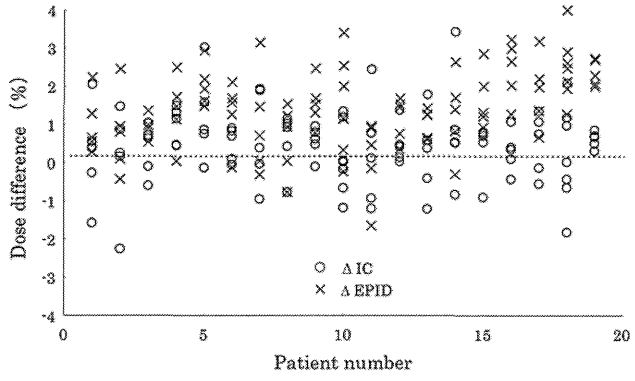

Fig. 7 Point dose difference between PD and IC measurements for 19 prostate IMRT plans (97 beams). Each result was compared with calculated values. A *positive number* indicates that the measured dose was higher than the calculated value

area. The maximum γ_{max} and γ_{avg} of the 309 beams were 3.1 and 0.41, respectively. The average γ_{max} and γ_{avg} of the 309 beams were 1.37 ± 0.42 and 0.26 ± 0.11, respectively. There were 10 fields (3.2 %) with errors of γ_{max} >2.0. In these fields, the measured doses were 6–18 % lower than the calculated dose at small points.

4 Discussion

The present study demonstrated that a PD system could be used for verification of IMRT dose delivery. First, the dosimetric properties of a-Si EPID were investigated. The acquisitioned frame rate was measured, and the acquisition frame number per MU was stable at 3 MU or more for both dose rates (Fig. 2b). The previous image acquisition CPU (IAS2) had a delay between each acquired image due to transfer of the image from the acquisition CPU to the disk and database [15]. This delay (i.e., dead time) was not fixed and could be more than 2.0 s. This delay resulted in image lag (i.e., loss of EPID signal) and inaccurate verification results. The IAS3 performance was different from that of the previous version, and there was no image lag during acquisition. Nonlinearity of the EPID response to MUs was observed in the low-MU region of this portal dosimetry system (Fig. 3). This was consistent with previous reports suggesting that the nonlinearity (known as ghosting effect) depends on the exposure and/or acquisition time [27–29]. The acquisition time dependence or ghosting effects are fundamental properties of the a-Si based EPID.

The calculation accuracy of the PDP algorithm was also investigated. The calculated CU was underestimated in a range of <70 MU. However, in a range of more than 70 MU, the differences between measured and calculated values were within 0.5 %. This result could be due to the fact that the EPID dose calibration was performed at 100 MU. Inaccuracy of the PD in a range of <70 MU may be attributed to a poor EPID response due to ghosting effects in the small-MU region.

Dose-rate fluctuations can occur during IMRT delivery; therefore, it is important to confirm the effect of dose rate fluctuations in PD. Intensity-modulated stepwise test patterns were delivered at 100 and 600 MU/min. Although the dose rate was stable during irradiation at 100 MU/min, it fluctuated between 130 and 600 MU/min when the leaf speed reached 2.5 cm/s. There was no difference in measured CUs at the two dose rates of 100 and 600 MU/min (Fig. 5), which means that dose-rate fluctuation did not affect the PD system.

Modeling of the MLC was commissioned with use of the IMRT test pattern shown in Fig. 1. T&G effects caused

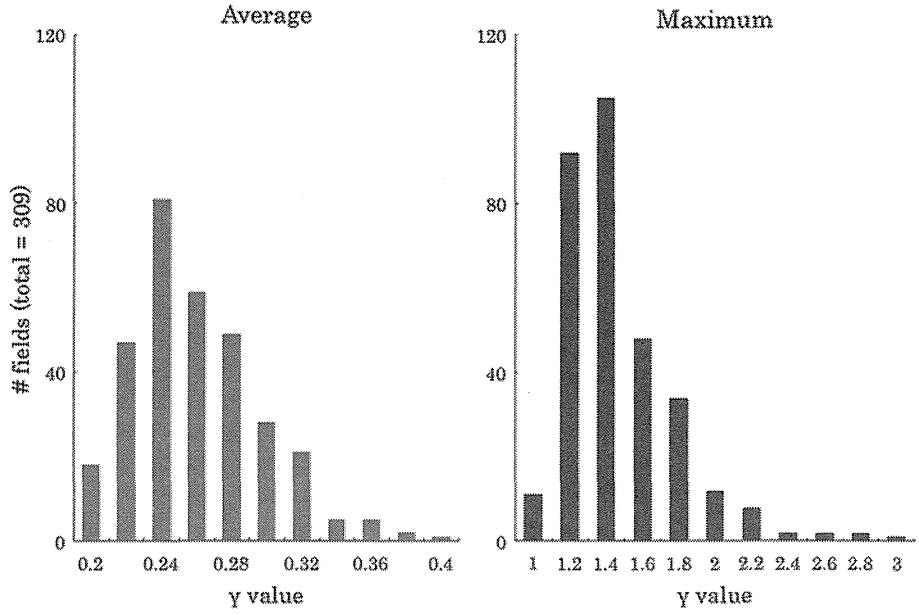

Fig. 8 Histogram of average and maximum γ values with use of 3 mm and 3 % tolerance, for 309 IMRT prostate fields. Measured and calculated dose distributions agreed well overall, with average $\gamma = 0.26$, and maximum $\gamma = 3.0$

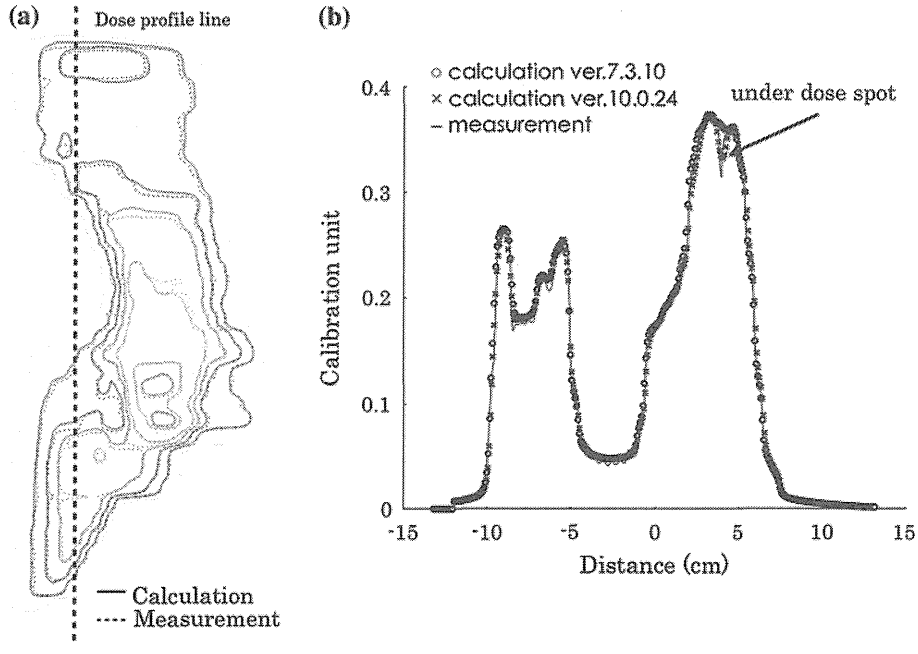

Fig. 9 Results of prostate IMRT verification by use of PDP calculation algorithm versions 7.3.10 and 10.0.24. **a** Measured and calculated dose distribution. *Solid lines* and *dashed lines* are calculation (PDP calculation algorithm version 7.3.10) and measurement, respectively. **b** Comparison of three dose profiles along with the *bold dashed line* in **a**

a large under dosage, and the maximum dose difference was above 20 % in this particular case (Fig. 6). Similar results were observed in our past film measurements. PDP algorithm version 7.3.10 could not calculate the PDI including T&G effects; thus, the gamma value increased when intensity-modulated beams had a single leaf movement. A large discrepancy from T&G effects was occasionally observed in the results of clinical IMRT verification, and an example is shown in Fig. 9. This IMRT treatment plan was used for prostate cancer with metastases of lymph nodes in the pelvis. This plan, therefore, had a large field and more complex leaf movement than ordinary prostate IMRT treatment plans. An under-dose spot was detected in PD, although no under-dose spot was observed in the dose distribution calculated by PDP algorithm version 7.3.10 (Fig. 9b). However, with the PDP calculation algorithm version 10.0.24, T&G effects in PDI can be calculated. T&G effects appear as a line shape moving in the direction of the MLC. Because under-dose spots due to T&G effects can be present in clinical treatment beam delivery, detection of T&G effects is important for quality control of IMRT.

The clinical applicability of PD was investigated with use of clinical IMRT beams for prostate cancer. The point

dose ratios of ΔIC and ΔEPID were 0.5 ± 0.9 % (average ± SD) and 1.4 ± 1.0 %, respectively, with the difference being significant. Although $EPID_{meas}$ was slightly higher than PDI_{calc}, the difference was acceptable clinically. This result suggested that PD is applicable for IMRT verification with the same accuracy as that of IC measurement. As a clinical application of PD, 309 prostate IMRT beams were verified. PDI calculated by PDP algorithm version 7.3.10 was used. The average values of γ_{max} and γ_{avg} were 1.37 ± 0.42 and 0.26 ± 0.11, respectively. Similar values of γ_{max} and γ_{avg} were reported for one PD study [30], and these values seem clinically acceptable. Although 10 fields of γ_{max} >2.0 were noted in the present study, γ_{max} exceeded 2.0 only in a small portion of the fields. Recalculation with PDP calculation version 10.0.24 was performed for the 10 fields, and the maximum gamma value of all 10 fields became γ_{max} <2.0. As the T&G effect was considered in the PDP calculation with version 10.0.24, a more accurate dose distribution was obtained compared with that for PDP algorithm version 7.3.10. Thus, the average gamma values in the present study were within a clinically acceptable range. Our PD system for each IMRT field dose distribution is useful in clarifying the reasons for any error.

In terms of the working time for verification of IMRT, it usually took 5 or 6 h to perform pretreatment IMRT verification with conventional film and IC measurements in our department. After we adopted the PD system, analysis of one clinical IMRT plan could be performed within 30 min. The waiting time between CT scanning for the treatment plan and the start of IMRT was also shortened, from 7 to 4 days.

5 Conclusion

Portal dosimetry including calibration, measurement, and analysis of one clinical IMRT plan could be performed within 30 min; this has a significant positive impact in a busy clinical environment. The PD system is a useful and fast method of dosimetry for both medical staff and patients.

Acknowledgments This study was supported in part by a Grant-in-Aid for Clinical Cancer Research (H23-009) from the Ministry of Health, Labour and Welfare of Japan, and by the National Cancer Center Research and Development Fund (23-A-21).

References

1. Xia P, Verhey LJ. Multileaf collimator leaf sequencing algorithm for intensity modulated beams with multiple static segments. Med Phys. 1998;25(8):1424–34.
2. Convery DJ, Webb S. Generation of discrete beam-intensity modulation by dynamic multileaf collimation under minimum leaf separation constraints. Phys Med Biol. 1998;43(9):2521–38.
3. Spirou SV, Chui CS. Generation of arbitrary intensity profiles by dynamic jaws or multileaf collimators. Med Phys. 1994;21(7):1031–41.
4. Stein J, Bortfeld T, Dorschel B, Schlegel W. Dynamic X-ray compensation for conformal radiotherapy by means of multi-leaf collimation. Radiother Oncol. 2004;32(2):163–73.
5. Wang X, Spirou S, LoSasso T, Stein J, Chui CS, Mohan B. Dosimetric verification of intensity-modulated fields. Med Phys. 1996;23(3):317–27.
6. Bucciolini M, Buonamici FB, Casati M. Verification of IMRT fields by film dosimetry. Med Phys. 2004;31(1):161–8.
7. Ju SG, Ahn YC, Huh SJ, Yeo IJ. Film dosimetry for intensity modulated radiation therapy: dosimetric evaluation. Med Phys. 2002;29(3):351–5.
8. Jursinic PA, Nelms BE. A 2-D diode array and analysis software for verification of intensity modulated radiation therapy delivery. Med Phys. 2003;30(5):870.
9. Poppe B, Blechschmidt A, Djouguela A, Kollhoff R, Rubach A, Willborn KC, et al. Two-dimensional ionization chamber arrays for IMRT plan verification. Med Phys. 2006;33(4):1005–15.
10. Looe HK, Harder D, Ruhmann A, Willborn KC, Poppe B. Enhanced accuracy of the permanent surveillance of IMRT deliveries by iterative deconvolution of DAVID chamber signal profiles. Phys Med Biol. 2010;55(14):3981–92.
11. Poppe B, Looe HK, Chofor N, Ruhmann A, Harder D, Willborn KC. Clinical performance of a transmission detector array for the permanent supervision of IMRT deliveries. Radiother Oncol. 2010;95(2):158–65.
12. Yin FF, Schell MC, Rubin P. Input/output characteristics of a matrix ion-chamber electronic portal imaging device. Med Phys. 1994;21(9):1447–54.
13. Zhu Y, Jiang XQ, Van Dyk J. Portal dosimetry using a liquid ion chamber matrix: dose response studies. Med Phys. 1995;22(7):1101–6.
14. Essers M, Hoogervorst BR, van Herk M, Lanson H, Mijnheer BJ. Dosimetric characteristics of a liquid-filled electronic portal imaging device. Int J Radiat Oncol Biol Phys. 1995;33(5):1265–72.
15. Greer PB, Popescu CC. Dosimetric properties of an amorphous silicon electronic portal imaging device for verification of dynamic intensity modulated radiation therapy. Med Phys. 2003;30(7):1618–27.
16. Greer PB. Correction of pixel sensitivity variation and off-axis response for amorphous silicon EPID dosimetry. Med Phys. 2005;32(12):3558–68.
17. Greer PB, Vial P, Oliver L, Baldock C. Experimental investigation of the response of an amorphous silicon EPID to intensity modulated radiotherapy beams. Med Phys. 2007;34(11):4389–98.
18. Greer PB, Barnes MP. Investigation of an amorphous silicon EPID for measurement and quality assurance of enhanced dynamic wedge. Phys Med Biol. 2007;52(4):1075–87.
19. McCurdy BMC, Greer PB. Dosimetric properties of an amorphous-silicon EPID used in continuous acquisition mode for application to dynamic and arc IMRT. Med Phys. 2009;36(7):3028–38.
20. Gustafsson H, Vial P, Kuncic Z, Baldock C, Denham JW, Greer PB. Direct dose to water dosimetry for pretreatment IMRT verification using a modified EPID. Med Phys. 2011;38(11):6257–64.
21. Sharma DS, Mhatre V, Heigrujam M, Talapatra K, Mallik S. Portal dosimetry for pretreatment verification of IMRT plan: a comparison with 2D ion chamber array. J Appl Clin Med Phys. 2010;11(4):238–48.

22. Warkentin B, Steciw S, Rathee S, Fallone BG. Dosimetric IMRT verification with a flat-panel EPID. Med Phys. 2003;30(12): 3143–55.
23. Wendling M, Louwe RJW, McDermott LN, Sonke J–J, van Herk M, Mijnheer BJ. Accurate two-dimensional IMRT verification using a back-projection EPID dosimetry method. Med Phys. 2006;33(2):259–73.
24. LoSasso T, Chui CS, Ling CC. Physical and dosimetric aspects of a multileaf collimation system used in the dynamic mode for implementing intensity modulated radiotherapy. Med Phys. 1998;25(10):1919–27.
25. Arnfield MR, Siebers JV, Kim JO, Wu Q, Keall PJ, Mohan R. A method for determining multileaf collimator transmission and scatter for dynamic intensity modulated radiotherapy. Med Phys. 2000;27(10):2231–41.
26. Low DA, Harms WB, Mutic S, Purdy JA. A technique for the quantitative evaluation of dose distributions. Med Phys. 1998; 25(5):656–61.
27. McDermott LN, Louwe RJW, Sonke JJ, van Herk MB, Mijnheer BJ. Dose–response and ghosting effects of an amorphous silicon electronic portal imaging device. Med Phys. 2004;31(2):285–95.
28. Winkler P, Hefner A, Georg D. Dose-response characteristics of an amorphous silicon EPID. Med Phys. 2005;32(10):3095–105.
29. McDermott LN, Nijsten SMJJG, Sonke JJ, Partridge M, van Herk M, Mijnheer BJ. Comparison of ghosting effects for three commercial a-Si EPIDs. Med Phys. 2006;33(7):2448–51.
30. Roxby KJ, Crosbie JC. Pre-treatment verification of intensity modulated radiation therapy plans using a commercial electronic portal dosimetry system. Australas Phys Eng Sci Med. 2010; 33(1):51–7.

Journal of Radiation Research, 2013, 54, 98–107
doi: 10.1093/jrr/rrs071 Advance Access Publication 24 August 2012

Alternating chemoradiotherapy in patients with nasopharyngeal cancer: prognostic factors and proposal for individualization of therapy

Yoko GOTO*, Takeshi KODAIRA, Nobukazu FUWA, Nobutaka MIZOGUCHI, Rie NAKAHARA, Motoo NOMURA, Natsuo TOMITA and Hiroyuki TACHIBANA

Department of Radiation Oncology, Aichi Cancer Center Hospital, 1-1 Kanokoden, Chikusa-ku, Nagoya 464-8681, Japan
*Corresponding author. Tel: +81-75-753-9301; Fax: +81-75-771-9749; Email: ygoto@kuhp.kyoto-u.ac.jp

(Received 19 May 2012; revised 15 July 2012; accepted 17 July 2012)

The purpose of this study is to assess the efficacy of alternating chemoradiation in patients with nasopharyngeal cancer. From 1990–2006, 100 patients with nasopharyngeal cancer were treated with alternating chemoradiation at the Aichi Cancer Center. Of these, 4, 2, 23, 34, 13 and 23 patients were staged as I, IIA, IIB, III, IVA and IVB, respectively. The median radiation doses for primary tumors and metastatic lymph nodes were 66.6 Gy (range, 50.4–80.2 Gy) and 66 Gy (range, 40.4–82.2 Gy), respectively. A total of 82 patients received chemotherapy with both cisplatin and 5-fluorouracil (5-FU), while 14 patients received nedaplatin (CDGP) and 5-FU. With a median follow-up of 65.9 months, the 5-year rates of overall survival (OAS) and progression-free survival (PFS) were 78.1% and 68.3%, respectively. On multivariate analysis (MVA), elderly age, N3, and WHO type I histology proved to be significantly unfavorable prognostic factors of OAS. As for PFS, there were T4, N3, and WHO type I histology in MVA. Acute toxicities of hematologic and mucositis/dermatitis ≥ Grade 3 were relatively high (32%); however, they were well-managed. Late toxicities of ≥ Grade 3 were three (3%) mandibular osteomyelitis and one (1%) lethal mucosal bleeding. Results for alternating chemoradiation for nasopharyngeal carcinoma are promising. In order to improve outcomes, usage of intensity-modulated radiation therapy and application of active anticancer agents are hopeful treatments, especially for groups with poor prognosis factors with WHO type I histopathology, T4 and/or N3 disease.

Keywords: nasopharyngeal carcinoma; alternating chemoradiation; WHO type I histopathology

INTRODUCTION

Nasopharyngeal carcinoma (NPC) is a common disease among Southern Chinese, Southeast Asian, Northern African and Inuit populations. In Japan, the USA and Western European countries it is relatively rare. Because of anatomical characteristics, surgical treatment is very difficult. In addition, the majority of NPC patients revealed undifferentiated carcinoma, which is relatively sensitive to radiation therapy. Therefore, radiotherapy is widely accepted as the first choice of therapy for NPC. In recent years, by randomized-control trials, chemoradiotherapy has shown significant survival benefits over radiotherapy alone, improving both local and distant control [1–4]. In addition, meta-analysis of eight randomized trials showed significant benefits for OAS and event-free survival [5]. The pooled hazard ratio of death was 0.82 (95% confidence interval, 0.71–0.94; $P = 0.006$), corresponding to an absolute survival benefit of 6% at 5 y from the addition of chemotherapy. Thus, the standard treatment for locally advanced NPC is now believed to be concurrent chemoradiotherapy. However, several key factors need further clarification. Firstly, the chemotherapy used in the Intergroup 0099 study (IGS) consisted of three courses each of concurrent administration of cisplatin (CDDP) and adjuvant chemotherapy with both CDDP and 5-fluorouracil (5-FU). However, about two thirds (63%) of patients could receive concurrent chemotherapy, and about half (55%) could receive the full course of adjuvant chemotherapy. Secondly, a higher incidence of adverse events ≥ Grade 3 was observed in the chemoradiation group than in the radiation alone group (59% vs 34%). Finally, chemoradiation reduced distant metastasis; however, it did not reach sufficient levels. Of the 18 patients with recurrence in the

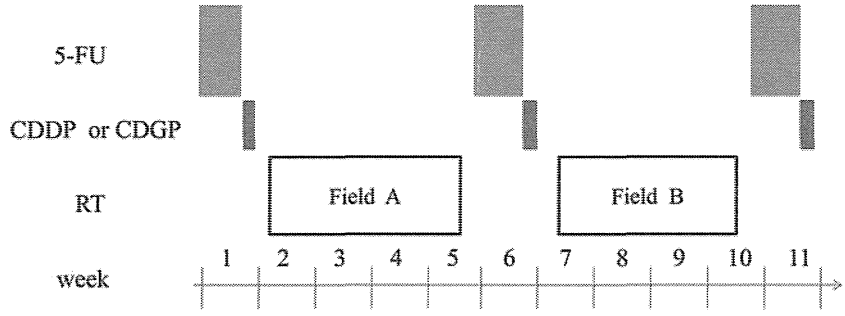

Fig. 1. Study design of alternating chemoradiotherapy. 5-FU = 5-fluorouracil 800 mg/m^2 on Days 1–5 continuous infusion, CDDP = cisplatin 50 mg/m^2 Day 6–7, CDGP = nedapatin 130 mg/m^2 on Day 6, RT = radiotherapy, Field A = large field including from the skull base to supraclavicular fossa, Field B = boost field including the nasopharynx and metastatic lymph nodes.

chemoradiation arm, 10 (56%) developed distant metastasis (DM) in the IGS. A considerable incidence of DM still developed in the IGS due to insufficient dose intensities of chemotherapy, instead of increasing adverse events.

In the Aichi Cancer Center, we conducted alternating chemoradiotherapy for advanced NPC patients from 1987 and reported promising results with sufficiently better compliance (94%), of which the 5-year OAS and PFS rates were 75% and 63%, respectively [6]. In the present study, we analysed the efficacy of alternating chemoradiotherapy for NPC with relatively longer follow-up and sought to refine our treatment strategy according to data regarding failure patterns.

MATERIALS AND METHODS

Patient characteristics

Between 1990 and 2006, a total of 100 consecutive patients with newly diagnosed histology-proven nasopharyngeal carcinoma underwent definitive chemoradiotherapy (CRT) in the Aichi Cancer Center. All patients underwent fiberoptic nasopharyngoscopy and magnetic resonance imaging (MRI) to assess the extent of primary and cervical lymph nodes. Evaluation of distant metastasis was done by chest X-ray, computed tomography (CT), liver ultrasonography, and bone scintigraphy. After 2002, positron emission tomography (PET) or PET-CT was also used to evaluate the extent of the disease. In addition, laboratory data, electrocardiograms, and 24-h creatinine clearance were evaluated to assess general condition. For this analysis, all patients were restaged according to the 6th edition of the American Joint Committee on Cancer (AJCC) staging system [6].

Treatment schedule

Chemotherapy

The treatment scheme is shown in Fig. 1. Details of the treatment regimen have been reported in another article [7]. Chemotherapy regimens were a combination of CDDP and 5-FU (FP) or nedaplatin (CDGP) and 5-FU (FN) regimens. In the FP regimen, 5-FU was administered continuously at a dose of 800 mg/m^2 on Days 1–5 and CDDP at a dose of 50 mg/m^2 on Days 6–7. In the FN regimen, 5-FU was administered continuously at a dose of 800 mg/m^2 on Days 1–5 and CDGP at a dose of 130 mg/m^2 on Day 6. Chemotherapy was performed in principal three times at 4-week intervals. However, when a WBC count <3000/mm^2 or a platelet count <100 000/mm^2 was obtained at the scheduled date of drug administration, chemotherapy was postponed and radiation therapy was alternately prescribed. When hematological data obtained two weeks after radiotherapy did not meet the inclusion criteria (WBC count >3000/mm^2 and platelet count >100 000/mm^2), the next cycle of chemotherapy was withdrawn. When the WBC count decreased to <1000/mm^2 or the platelet count decreased to <25 000/mm^2 after chemotherapy, doses of both 5-FU and CDDP were decreased by 25% at the next cycle. In addition, the dose of CDDP only was decreased by 25% when serum creatinine levels >1.5 mg/dl were noted.

Radiotherapy

Using a 6–10 MV photon beam by linear accelerator, external beam radiotherapy commenced 2–3 d after the completion of previous chemotherapy. At simulation and daily treatment, the head, neck and shoulder were immobilized in a hyperextended position using a thermoplastic mask. Radiotherapy was performed with a daily fraction of 1.8–2.0 Gy. The initial radiation field covered the nasopharynx and upper and middle cervical regions using bilateral opposing portals and lower cervical, and supraclavicular region using anterior single field irradiation at a dose of 36–40 Gy. Then, a shrinking field of 26–30 Gy was boosted to the nasopharynx and involved lymph nodes using the dynamic conformal rotational technique. In the shrinking field, we kept enough margins of primary tumors and involved lymph nodes from the edge of field. Those margins were mainly decided dependent on proximity to

critical structures such as the brain-stem, spinal cord, optic pathway and temporal lobes. During the second period of chemotherapy, radiotherapy was temporarily interrupted to spare the increasingly acute toxicity of 5-FU. Additional boosts of up to 10 Gy with stereotactic multiple arc treatment were also permitted, if residual tumors existed at primary sites.

Follow-up and statistical consideration

Toxicities of CRT were evaluated according to the Common Terminology Criteria for Adverse Events (CTCAE) version 3.0 [8]. During the treatment period, complete blood counts and biochemical examinations were performed at least once a week. After completion of CRT, the treatment response was assessed by fiberoptic nasopharyngoscopy, MRI and/or PET/CT. The frequency of follow-up was every month for the first year, once every two months between the second and third post-treatment year, and once every three months after the third post-treatment year. Fiberoptic nasopharyngoscopy was performed at every visit, and post-treatment MRI scans were obtained every three months for the first year and then every six months thereafter. The survival period was calculated from the start of treatment to death or the last follow-up examination, and progression-free survival was defined as the period from the start of treatment to the progression of tumors or death by any cause. Overall survival and progression-free survival curves were calculated by the Kaplan-Meier method [9]. The log-rank test was used to compare survival curves. A Cox-proportional hazard model was used for multivariate analysis. Differences in the ratios between the two groups were assessed by the chi-square test.

RESULTS

Patient characteristics

Between June 1990 and March 2005, 100 patients with NPC received definitive CRT in the Aichi Cancer Center. Table 1 shows patient characteristics in this cohort. We analysed all patients who were treated with CRT. The median age was 55 years old (range, 28–80). Performance status was distributed as 2 of 0, 93 of 1, 3 of 2, and 2 of 3, respectively. Of these, 8 patients (8%) had histopathology with keratinizing squamous cell carcinoma (WHO type I), and 70 patients (70%) had Stage III–IVB disease. During this period the number of patients with NPC who were treated with radiotherapy alone was 13. The common reasons for radiotherapy alone were advanced age or poor general condition.

Table 1. Patient characteristics

Characteristics			*n*
Age, years: median (range)		55 (28–80)	
Gender:			
	Male		72
	Female		28
Performance status			
		0	2
		1	93
		2	3
		3	2
Histology			
		type I	8
		non type I	90
		others	2
T stage			
		1	37
		2a	15
		2b	15
		3	15
		4	18
N stage			
		0	11
		1	31
		2	34
		3a	9
		3b	15
Stage			
		I	4
		IIA	2
		IIB	24
		III	34
		IVA	12
		IVB	24

Treatment contents

The median dose to the primary site was 66.6 Gy (range, 50.4–80.2 Gy), and the median dose to involved lymph nodes was 66 Gy (range, 40.4–82.2 Gy), respectively. The median period of the whole course of alternating CRT was

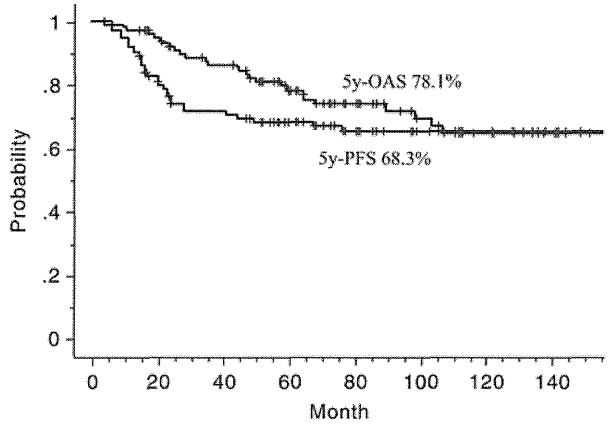

Fig. 2. Overall survival (OAS) and progression-free survival (PFS) curves.

85 days (range, 47–147 days), and the median period of overall treatment time of radiation therapy (OTT) was 69 days (range, 42–110 days).

Treatment outcomes

The 5-year rates of OAS and PFS were 78.1% and 68.3%, respectively (Fig. 2). The 5-year rates of OAS of the group divided by stage were 100, 100, 86.1, 77.6, 91.7 and 60.3% for Stage I, IIA, IIB, III, IVA and IVB, respectively. The 5-year rates of OAS and PFS of 96 patients who received alternating CRT were 78.2% and 68%, respectively. As for initial response after completion of CRT, complete remission (CR) rates of primary and nodal lesions were 86% and 83%, respectively. At a median follow-up of 65.9 months (range, 3.9–22.9 months), 62 were alive without disease, 11 were alive with disease, 18 died from the disease, 2 died from other diseases (both esophagus carcinoma) and 7 died from unknown reasons.

The 5-year rates of loco-regional progression-free survival (LRPFS) and distant metastasis-free survival (DMFS) were 77.9% and 87.8%, respectively.

A total of 32 patients (32%) developed treatment failure at one or more sites. Disease progression developed in 19 for primary, 9 for regional and 11 for distant sites at the last follow-up. Among 11 patients with distant failure, the most frequent site was the lung in 8, followed by bone in 4 and the liver in 2.

Of 21 patients who developed locoregional recurrence, 13 were treated with additional chemoradiation. Of the remainder, 2 patients were re-treated with radiotherapy alone, and 4 with only chemotherapy. One patient received neck dissection for regional failure, and another did not receive any treatment because of the patient's refusal for treatment.

Out of 11 patients who developed distant metastasis, 9 were treated by chemotherapy, and 2 patients received palliative radiotherapy only.

Univariate analysis

Univariate analysis (UVA) results are listed in Table 2.

Elderly age, male, WHO type I histology, and N3 were revealed as significant unfavorable prognostic factors of OAS. The 5-year rate of OAS of the group with WHO type I histology was significantly lower than that with non-type I histology (33.3% vs 81.6%, $P < 0.0001$, Fig. 3). The group with N3 lesions had significantly worse 5-year OAS (60.3%) than that with N0–2 (84%; $P = 0.0017$). The 5-year rates of OAS of patients who received reduced dose and planned dose chemotherapy were 76.6% and 78.6%, respectively ($P = 0.75$).

As for PFS, significantly unfavorable factors were revealed as WHO type I histology, T4 and N3.

The 5-year PFS rate of the group with N3 was significantly lower than that with N0–2 (41.5% vs 76.5%, $P = 0.001$). The 5-year PFS rate of the group with T4 was significantly lower than that with T1–3 (54.5% vs 71.4%, $P = 0.014$). The 5-year rates of PFS of patients who received reduced dose and planned dose chemotherapy were 69.7% and 66.7%, respectively ($P = 0.59$).

The 5-year rate of LRPFS of the group with WHO type I histology was significantly lower than that with non-type I histology (21.4 % vs 84.5 %, $P < 0.0001$).

The 5-year rate of DMFS of patients with N3 was significantly lower than that with N0–2 (62.8% vs 95.1%, $P < 0.0001$). The 5-year LRPFS of patients with T4 was significantly lower than that with T1–3 (63.3% vs 81.1%, $P = 0.027$).

Multivariate analysis

Multivariate analysis (MVA) results are listed in Table 3. On MVA, significantly unfavorable prognostic factors of OAS were elderly age, WHO type I histology and N3, respectively. As for PFS, they were WHO type I histology, T4 and N3, respectively.

Treatment compliance

Regarding the contents of chemotherapy, 82 patients received FP, while 14 received FN. Four patients had other chemotherapy regimens, as described below. One patient with Stage I (cT1N0M0) received two courses of CDDP/5-FU followed by definitive radiotherapy. One patient received six courses of weekly docetaxel (TXT) because of elderly age and poor medical condition. One patient received chemotherapy with both CDGP and TXT because 5-FU was inappropriate due to a past history of myocardial infarction. One patient received concurrent administration with decreased doses of CDGP and 5-FU due to elderly age. Chemotherapy compliance is shown in Table 4. In 96 patients who received alternating CRT, over 90% of patients received three courses of chemotherapy and 70% of patients received the planned dose of three courses. In

Table 2. Univariate analyses for overall survival and progression-free survival

Factors	No.	5-year OAS (%)	*P*-value	5-year PFS (%)	*P*-value
Gender					
Female	28	88.7	0.017	77.9	0.15
Male	72	73.8		64.4	
Age (years)					
<51	48	93.4	0.0006	73.6	0.26
≥51	52	64.2		63.4	
PS					
0, 1	95	79.1	0.148	69.9	0.1
2, 3	5	60		30	
Histology					
WHO non type I	90	81.6	$P < 0.0001$	72.1	$P < 0.0001$
type I	8	33.3		14.3	
T stage					
T1–3	82	78.2	0.79	71.4	0.014
≥T4	18	77.4		54.5	
N stage					
N0–2	76	84	0.001	76.5	0.001
N3	24	60.3		41.5	
Total treatment duration (day)					
<85	48	69	0.0615	62.3	0.135
≥85	52	85.6		73.8	
OTT (day)					
<69	49	78.2	0.884	72.2	0.36
≥69	51	78.2		64.8	
Dose for primary site (Gy)					
<66	30	76.7	0.712	70	0.7
≥66	70	78.7		67.5	
Dose for metastatic LN (Gy)					
<66	35	77.5	0.683	71.8	0.78
≥66	54	74.8		65.1	

OAS = overall survival, PFS = progression-free survival, PS = performance status, WHO = World Health Organization, OTT = overall treatment time of radiotherapy, LN = lymph node.

detail, 29 patients received reduced dose chemotherapy while 67 patients received the planned dose of three courses. The most common reason for dose reductions was renal dysfunction (47%), followed by severe mucositis (20%). The median total dose of CDDP was 300 mg/m^2 (range, 150–340 mg/m^2), CDGP was 375 mg/m^2 (range, 80–400 mg/m^2), and for 5-FU was 12 000 mg/m^2 (range, 3050–12 000 mg/m^2). In the cohort of patients who received reduced dose chemotherapy, the median total doses of CDDP, CDGP and 5FU were 250 mg/m^2, 330 mg/m^2 and 9400mg/m^2, respectively. Unplanned interruption of RT was experienced in 14 patients (14%), and 2 out of 14 patients required a break in RT over seven days. Severe mucositis (36%) was the most common reason for interruption of RT, followed by infection of the hyperalimentation catheter (29%).

Treatment toxicity

Acute toxicities observed during treatment are listed in Table 5. The most common toxicity was leukopenia. Grade

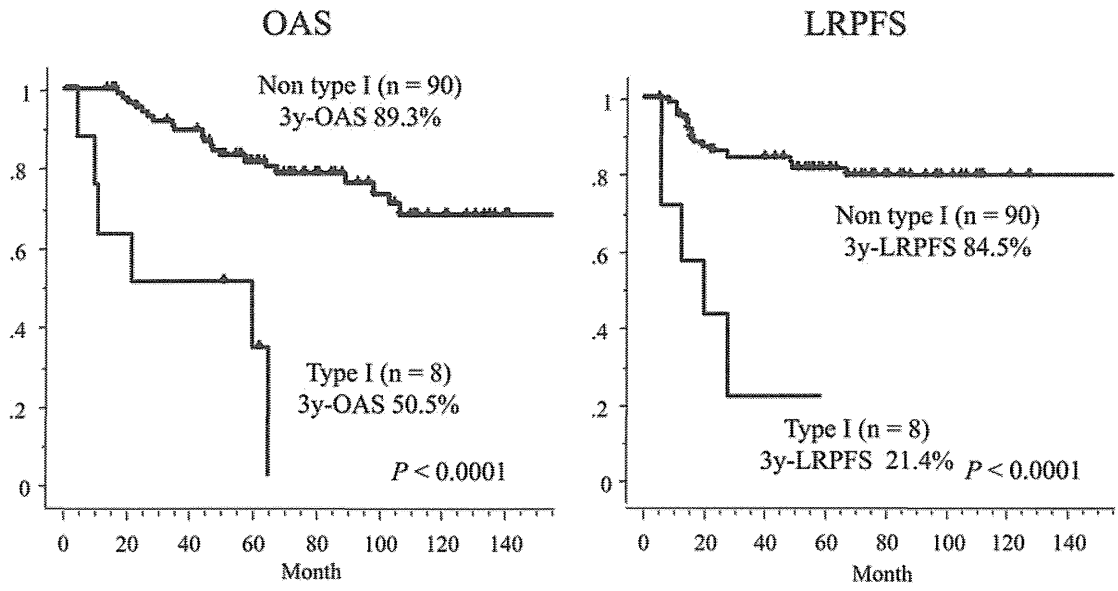

Fig. 3. Overall survival (OAS) and locoregional progression-free survival (LRPFS) curves of groups divided by WHO histopathological types.

Table 3. Multivariate analyses for overall survival and progression-free survival

		OAS		PFS	
Factors	**No.**	**HR (95% CI)**	***P*-value**	**HR (95% CI)**	***P*-value**
Gender					
Female	28		0.109		0.5
Male	72	2.76 (0.104–1.257)		1.36 (0.291–1.836)	
Age (years)					
<51	48		0.0018		0.198
≥51	52	4.92 (0.074–0.551)		1.62 (0.294–1.290)	
Histology					
WHO non type I	90		0.0034		0.0004
type I	8	4.62 (0.077–0.603)		5.747 (0.067–0.454)	
T stage					
T1–3	82		0.555		0.023
T4	18	1.36 (0.264–2.047)		2.5 (0.181–0.881)	
N stage					
N0–2	76		0.0076		0.0025
N3	24	3.03 (0.147–0.745)		3.012 (0.163–0.680)	
OTT (day)					
<69	49	1.10 (0.395–2.065)	0.8092		0.605
≥69	51			1.215 (0.393–1.724)	

HR = hazard ratio, CI = confidence intervals, OAS = overall survival, PFS = progression-free survival, WHO = World Health Organization, OTT = overall treatment time of radiotherapy.